

Oscillations and Decay of Superfluid Currents in a One-Dimensional Bose Gas on a Ring

Juan Polo^{1,2,*}, Romain Dubessy³, Paolo Pedri³, H el ene Perrin³, and Anna Minguzzi¹

¹*University Grenoble Alpes, CNRS, LPMMC, 38000 Grenoble, France*

²*Quantum Systems Unit, Okinawa Institute of Science and Technology Graduate University, Onna, Okinawa 904-0495, Japan*

³*Laboratoire de Physique des Lasers, CNRS, Universit  Paris 13, Sorbonne Paris Cit , 99 Avenue J.-B. Cl ment, F-93430 Villetaneuse, France*

 (Received 10 April 2019; revised manuscript received 22 July 2019; published 6 November 2019)

We study the time evolution of a supercurrent imprinted on a one-dimensional ring of interacting bosons in the presence of a defect created by a localized barrier. Depending on interaction strength and temperature, we identify various dynamical regimes where the current oscillates, is self-trapped, or decays with time. We show that the dynamics is captured by a dual Josephson model and involve phase slips of thermal or quantum nature.

DOI: [10.1103/PhysRevLett.123.195301](https://doi.org/10.1103/PhysRevLett.123.195301)

Superfluidity is a fascinating phenomenon emerging in interacting quantum systems and governing their low temperature transport properties. Supercurrents, named in analogy with superconductivity, are characterized (among others) by frictionless flow and quantized vortices; and they are most easily evidenced in ring geometries. Ultracold atoms confined in ring traps have proven to be a great tool to study superfluid transport properties [1–3]. Due to their tunability and their high degree of control, they are an ideal system for studying the effect of interactions and dimensionality in the superfluid transport dynamics. Because superconducting quantum interference devices have provided a wealth of applications, the realization of their atomic analogs—the atomtronic quantum interference device (AQUID) [4]—is an important step in the field of atomtronics [5–9].

From a fundamental point of view, an open question is the stability of supercurrents. This is related but complementary to the study of setting the superfluid in rotation, which is also related to vortex nucleation [10–12]. For a three-dimensional (3D) ring geometry, the stochastic decay of the quantized current has been studied, evidencing the role of the critical velocity [2,13]. In the presence of a repulsive barrier crossing the ring, resulting in a weak link, hysteresis in the phase slips’ dynamics has been investigated [14–18] and the role of thermal activation evidenced [19]. A scenario for the phase slips’ dynamics induced by a weak link based on the role of vortices can be used to explain qualitatively the experimental observations [20], but it fails to account quantitatively for the thermal activation [21,22]. Also, in a 3D fermionic double-well Josephson junction, phase slips play a role in the dynamics [23,24].

In this context, one question naturally arises: if the phase slips’ dynamics are driven in 3D by vortices crossing the weak link, what happens in lower dimensions?

Although, in two-dimensional (2D) systems, vortices still play a crucial role in the superfluid dynamics [4,20], they cannot exist in one dimension. Therefore, the phase slips’ phenomenon should be of a different nature in 1D.

Previous works have shown the role of phase slips [25,26] in the decay of 1D transport in the presence of periodic perturbation [27]. For a microscopic impurity, the decay rate has been estimated by computing the drag force [28]. For sufficiently small obstacles, stationary circulating states may exist [29–31], whereas a forced flow past a larger obstacle results in soliton emission [32–34]. Most of the previous studies were performed in a rotating frame, thus imposing a flow onto the ring, allowing us to estimate the nucleation rate of the phase slips [35]. For intermediate to strong interactions and small barriers, it has been shown that the decay of persistent currents is related to the low-energy excitations in the ring [36].

In this work, we investigate how a free current flows in 1D: as illustrated in Fig. 1, starting from a system initially prepared in a well-defined current state in a ring trap with a barrier, we follow the current dynamics with the aim of elucidating the dissipation mechanisms. Our study concerns both zero- and finite-temperature gases: both at weak and strong interactions. We show that the dynamical behavior can be interpreted as a dual of the Josephson effect occurring among angular momentum states. Depending on the barrier strength and the temperature regime, we observe current oscillations, self-trapping, or decay. In the weakly interacting regime, we show that the observed dynamics correspond to self-trapping among angular momentum states at zero temperature, and that the decay of the currents at finite temperature involves dark solitons. For strong interactions, we show that coherent quantum phase slips dominate the current dynamics at zero temperature, and incoherent ones take over at finite temperature.

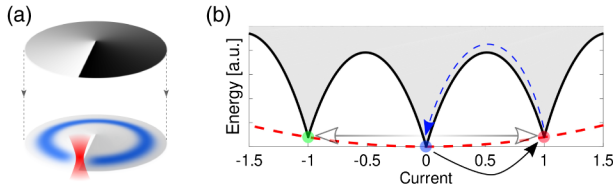


FIG. 1. (a) Sketch of the quench protocol: a one-dimensional (1D) Bose gas on a ring in the presence of a localized barrier; e.g., a tightly focused repulsive optical potential (red) creating a dip in the density (blue) is quenched out of equilibrium by phase imprinting. (b) Energy landscape of the homogeneous 1D Bose gas on a ring: states with integer values of the current per particle correspond to local minima of the energy. Quench (black arrow) transfers the system from the initial zero-current state (light blue circle) to the state with one unit of current (light red circle). Depending on the parameters, the barrier can resonantly couple the $+1$ and -1 states (light gray arrow) or induce an adiabatic transition between the $+1$ and 0 states (dashed blue arrow).

Model.—We consider N bosons of mass m with repulsive contact interactions on a ring of circumference L , with periodic boundary conditions (i.e., the Lieb-Liniger model) generalized to include the presence of an external barrier potential $V(x)$. The Hamiltonian reads

$$\hat{\mathcal{H}} = \int_0^L dx \hat{\Psi}^\dagger \left(-\frac{\hbar^2}{2m} \frac{\partial^2}{\partial x^2} + V(x) + \frac{g}{2} \hat{\Psi}^\dagger \hat{\Psi} \right) \hat{\Psi}, \quad (1)$$

where $\hat{\Psi}$ is the bosonic field operator; and $n = N/L$ is the average density, with a total number of particles of $N = \int_0^L dx \langle \hat{\Psi}^\dagger \hat{\Psi} \rangle$. This model describes, e.g., ultracold atoms confined in a tight ring trap. In this case, $g = 2\hbar\omega_\perp a_s$ is the 1D interaction strength, ω_\perp is the radial confinement frequency, and a_s is the 3D s -wave scattering length. In the following, we consider either a delta potential $V(x) = \alpha\delta(x)$, for which analytical results can be obtained, or a Gaussian potential $V(x) = V_0 \exp[-(x^2/2\sigma^2)]$, which is realistic from the experimental point of view. For homogeneous 1D gases, the equilibrium properties at finite temperature are captured by two dimensionless parameters [37]: $\gamma = mg/\hbar^2 n$, quantifying the interaction regime from weak ($\gamma \ll 1$) to strong ($\gamma \gg 1$); and the reduced temperature $\tau = T/T_d \gamma^2$, where $T_d = \hbar^2 n^2 / 2mk_B$ is the quantum degeneracy temperature.

Quench protocol.—Our goal is to study the dynamics of the particle current in the presence of a barrier. We first prepare the system in an equilibrium state Ψ_0 in the presence of the static barrier potential. This results in a state with no current. Specific details on the implementation depend on the interaction regime and are given later. We then quench the current by phase imprinting a specific circulation onto the many-body wave function:

$$\Psi_0(x_1, \dots, x_N) \rightarrow \Psi_1(x_1, \dots, x_N) = \Psi_0 \times e^{i2\pi\ell \sum_j x_j/L}.$$

Note that this process can be implemented in experiments by using specific light potentials according to various available schemes [2,38]. We then monitor the current by computing the average of the current operator per particle:

$$J(t) = -i \frac{\hbar}{2mN} \int_0^L \frac{dx}{L} \langle \hat{\Psi}^\dagger \partial_x \hat{\Psi} - (\partial_x \hat{\Psi}^\dagger) \hat{\Psi} \rangle. \quad (2)$$

The time evolution following the quench is described by different approaches, depending on the interaction and temperature regimes: (i) at $T = 0$ and for a weakly interacting gas ($\gamma \ll 1$), we rely on the Gross-Pitaevskii (GP) equation numerical solution and on an analytical two-mode model adapted from [39]; (ii) at $T > 0$ and $\gamma \ll 1$, we use the projected Gross-Pitaevskii equation formalism [40–42]; and (iii) at $\gamma \gg 1$, we use an exact time-dependent Bose-Fermi mapping describing the infinitely strong interaction Tonks-Girardeau (TG) limit for the whole temperature range [43–45], focusing on a quench with circulation $\ell = 1$ [46].

In the weakly interacting limit, we scale the Gaussian barrier strength relative to the chemical potential; i.e., we define $\lambda_{\text{GP}} = V_0/\mu_0$ with $\mu_0 = gn$ as the chemical potential of the homogeneous annular gas. Figure 2 illustrates our simulation results in the weakly interacting regime as a function of λ_{GP} for a relatively narrow barrier of width $\sigma = L/50$; yet, it is larger than the healing length $\xi = \hbar/\sqrt{2mgn} \simeq \sigma/4$. At zero temperature, we observe in Fig. 2(a) that the current remains very close to the initial quenched circulating state for weak to moderate barriers: up to $\lambda_{\text{GP}} \sim 1$. Above this critical value, we observe a fast decay of the current, followed by oscillations around the zero value. This is very similar to what has been obtained in 2D simulations [21]. The new feature of the 1D mean-field regime is the emergence of current oscillations at large barriers. As we will discuss here in the following, this behavior can be interpreted as the transition from self-trapping to Josephson oscillations of the currents, which is in analogy to the well-known Josephson effect for particle imbalance predicted in [39] and experimentally observed using ultracold atoms confined in a double-well trap [47]. In essence [48], we derive a fully analytical two-mode model for two current states and show that this accurately captures the Gross-Pitaevskii dynamics at zero temperature and very weak interactions [see Fig. 2(c)]. This model predicts a transition from self-trapping to Josephson oscillations for a critical value λ_{GP}^c that depends on the interaction strength as in [39]. Interestingly, a two-mode model based on current states in the linear regime also accurately describes the dynamics of vortex nucleation in stirred condensates [57]. Although the two-mode model breaks down for large barrier or higher (but still weak) interactions due to the spread of the mean-field wave function onto many single particle orbitals, we observe

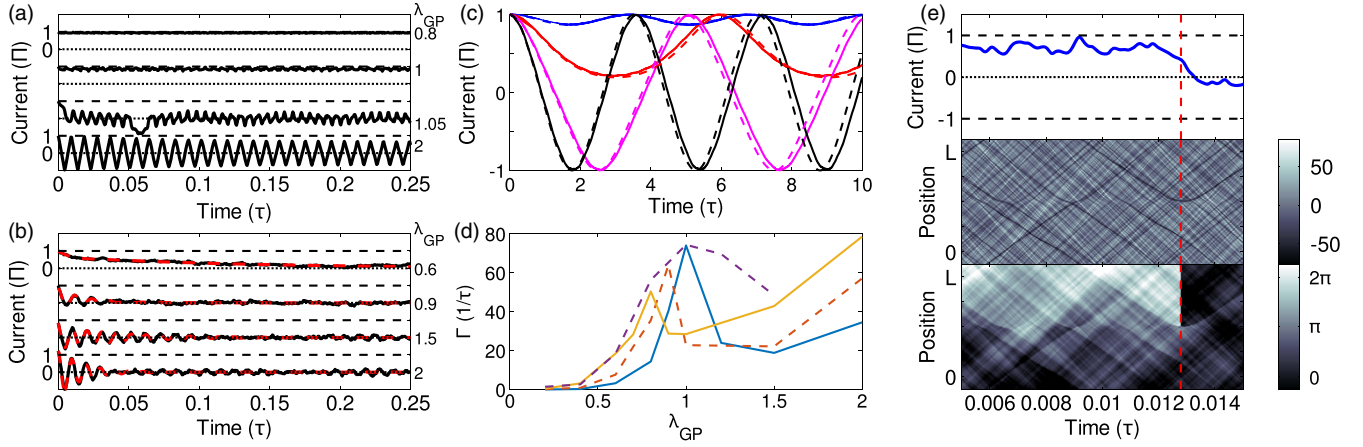


FIG. 2. Classical field simulations of the quench dynamics in the mean-field regime for $g = 20 \times \hbar^2/(mL)$ and $N = 1000$ (corresponding to $\gamma = 0.02$). (a) Average current per particle (black solid lines, in units of $\Pi = \hbar/(Nm)$) as a function of time (in units of $\tau = mL^2/\hbar$), at $T = 0$. The horizontal black dotted (dashed) lines indicate the values $J = 0$ (± 1). From top to bottom, $\lambda_{GP} = \{0.8, 1, 1.05, 2\}$. (b) Current at $T = \mu_0/k_B$, averaged over 100 realizations of the classical field, for barrier strengths $\lambda_{GP} = \{0.6, 0.9, 1.5, 2\}$, where black solid lines indicate simulations and red dashed curves indicate fits from the model function $J(t) = Ae^{-\Gamma_A t} + B \cos[\omega t + \phi]e^{-\Gamma_B t}$. (c) Current for $\gamma = 2 \times 10^{-5}$ at $T = 0$ simulations (solid lines) and two-mode model (dashed lines) for $\lambda_{GP} = \{0.05, 0.1, 0.15, 0.2\}$ (blue, red, magenta, and black, respectively). (d) Damping rate Γ (in units of $1/\tau$) (extracted from the fit, with a maximum among Γ_A and Γ_B) as a function of λ_{GP} for $T = \{0.5, 1, 1.5, 1.75\} \times \mu_0/k_B$ (solid blue, dashed red, solid yellow, and dashed violet, respectively). (e) Zoomed-in view of a single classical field trajectory, at $T = \mu_0/k_B$ and $\lambda_{GP} = 0.6$, evidencing a phase slip: a jump in the current (top panel) corresponds to the reflection of a slow soliton at the barrier, which is visible in the density deviation map [58] (middle panel) and to a singularity in the phase profile (bottom panel).

the same qualitative behavior in the simulations. Indeed, surprisingly, the current always oscillates regularly at large barriers [bottom curve of Fig. 2(a)], with a nonsinusoidal (piecewise linear) shape and a very small damping rate. These oscillations can be understood by casting the GP equation into the superfluid hydrodynamic form: transport of matter occurs via a density fluctuation corresponding to a shock wave [32], propagating at the speed of sound on top of a moving fluid.

For a temperature of $T = \mu_0/k_B$, corresponding to the quasicondensate regime [37], the dynamics of the current are quite different from the zero-temperature case; see Fig. 2(b). At low barriers (i.e., $\lambda_{GP} \leq 0.5$), we observe an exponential decay of the current with a decay rate increasing with the barrier strength. For larger barriers, we observe damped oscillations of the current. In this regime, thermal phase slips occur deterministically at the position of the barrier, where the density vanishes. The transition from exponential to damped oscillation decay is observed for all our temperatures in the range $0.5 \leq k_B T/\mu_0 \leq 2.5$. Figure 2(d) displays the value of the damping rate Γ given by the fit [59] for increasing temperatures, in the range of $0.5 \leq k_B T/\mu_0 \leq 1.75$. The damping rate increases with temperature, displaying a nonmonotonic dependence on the barrier strength, with a maximum at the crossover between the two decay regimes. The crossover occurs at lower barrier strength for larger temperatures, which is consistent with the thermal activation of solitons, as we will discuss below.

In order to elucidate the mechanisms for the current decay, Fig. 2(e) shows a single classical field trajectory, showing many spontaneous thermal gray solitons [60]. Although most of the solitons present a small density dip, and hence are fast and are transmitted through the barrier [61], we notice that the current undergoes discrete jumps each time a soliton is reflected on the barrier: in this case, when the soliton reaches zero velocity, the density profile vanishes, allowing for a phase slip to occur. This corresponds to the adiabatic process indicated by the dashed blue line on Fig. 1(b). As the temperature increases, the probability of finding slow solitons increases and the jumps occur more and more frequently, resulting in an increase of the decay rate, as seen in Fig. 2(d). Finally, as the barrier couples the soliton dynamics to the long wavelength sound excitations [61], we expect this process to be intrinsically stochastic, thus resulting in an exponential decay of the average current as observed.

The description of current dynamics as dual of the Josephson effect persists at strong interactions. In this regime, the classical picture does not apply; rather, we show below that the dynamics correspond to quantum coherent oscillations among angular momentum states (see [62] for the analog phenomenon in superconductors). We describe the dynamics of the current in the strongly interacting limit $\gamma \gg 1$ using the exact Tonks-Girardeau solution, which maps the interacting bosons onto a Fermi gas. In the TG regime, the relevant dimensionless barrier strength is $\lambda_{TG} = V_b/E_F$, with $V_b = an$ being the barrier

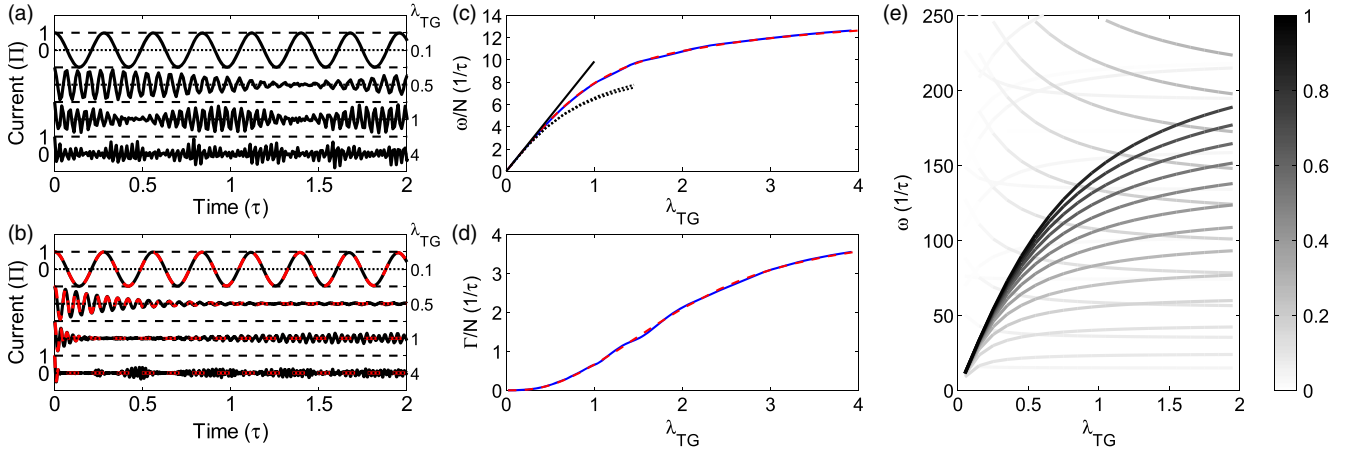


FIG. 3. Exact solutions in the Tonks-Girardeau regime. (a) Average current per particle (in units of $\Pi = \hbar/Nm$) vs time (in units of $\tau = mL^2/\hbar$) after the quench for $N = 23$, at $T = 0$, for barrier strength $\lambda_{\text{TG}} = \{0.1, 0.5, 1, 4\}$. The horizontal black dotted (dashed) lines indicate the values $J = 0 (\pm 1)$. (b) Current at $T = E_F/k_B$ (black solid) for $\lambda_{\text{TG}} = \{0.1, 0.5, 1, 4\}$ from top to bottom and fits (red dashes, with same fitting function as in Fig. 2). (c) Frequency ω/N , and (d) damping rate Γ/N obtained from the fit vs λ_{TG} for $N = 11$ (solid blue) and $N = 23$ (dashed red). Other curves in Fig. 3(c): frequency for universal Rabi oscillations $\omega_R = \pi^2 N \lambda_{\text{TG}}$ (black solid) and first excitation frequency at the Fermi sphere (black dashed) [48]. (e) Frequency of the excitations produced in the quench (relative amplitude in color map) vs λ_{TG} for $N = 23$ at $T = 0$.

associated energy and $E_F = \hbar^2 n^2 \pi^2 / 2m$ being the Fermi energy, corresponding to the zero-temperature chemical potential for systems displaying fermionization [48]. At zero temperature [Fig. 3(a)], we note that, for weak barriers, $\lambda_{\text{TG}} \ll 1$, which is in contrast to the weakly interacting regime: there is no self-trapping; rather, the current undergoes Rabi-like oscillations. These oscillations correspond to coherent quantum phase slips due to backscattering induced by the barrier, which breaks rotation symmetry, thus coupling different angular momentum states [6,30,63]. Microscopically, it corresponds to dynamical processes involving the whole Fermi sphere, i.e., multiple-particle hole excitations where each particle coherently undergoes oscillations of angular momentum from $L_z = \hbar$ to $L_z = -\hbar$. At increasing barrier strength, an envelope appears on top of the current oscillations, degrading the Rabi oscillations. This envelope originates from the population of higher-energy modes, with each transition being characterized by a different frequency [see Fig. 3(e) and [48]], leading to a mode-mode coupling and dephasing, and correspondingly more complex current oscillations.

At finite temperatures, the quench dynamics of the current involve high-energy excitations with the amplitude weighted by the Fermi distribution [48]. The resulting dynamics correspond to an effective damping of the current oscillations with an exponential decay [see Fig. 3(b)] corresponding to the effect of incoherent phase slips. The revivals observed for the large barrier at zero temperature are highly suppressed due to the thermal excitations. In Fig. 3(d), we show the decay rate Γ of the persistent currents as a function of the barrier strength [59]. We find that the decay of persistent currents grows monotonically

with the barrier strength because more and more excitations are involved in the dynamics as the barrier strength increases. In Fig. 3(c), we show the oscillation frequency as a function of λ_{TG} and observe that, at increasing barrier strength, the frequency crosses over from a Rabi-like regime with $\omega = \pi^2 N \lambda_{\text{TG}}$ to a Josephson-like regime with $\omega \propto \sqrt{\lambda_{\text{TG}}}$, which is in agreement with the predictions of the low-energy Luttinger liquid theory [36]. Quite generally, although our results have been derived for infinite interaction strength, the predictions of the TG model, including quantum fluctuations in an exact way, are expected to closely describe a Bose gas at strong interactions.

In conclusion, we have shown that the dynamical evolution following a phase imprinting induces oscillations of the current in a 1D ring, which are associated to a rich excitation pattern, which can be described by the dual Josephson dynamics. At weak interactions and a finite temperature, we observe the formation of both sound waves and of thermally activated dark solitons. We find that phase slippage occurs incoherently when the solitons are reflected by the barrier. In the strongly interacting regime at zero temperature, we find coherent Rabi oscillations indicating quantum coherent phase slips, which are degraded by mode dephasing at large barrier strength or by thermal fluctuations at finite temperature. In the weakly interacting limit, we find self-trapping of current states, whereas no self-trapping is found at infinitely strong interactions, where quantum fluctuations dominate.

The dual Josephson picture is a new paradigm for the dynamics of atomtronics circuits in which a current state encodes quantum information. Our work evidences the importance of the dynamics of the current in a 1D system,

which can be accurately measured using existing experimental tools: an interferometric measurement accessing the local currents [64,65] or long wavelength excitations [66,67]. The stochastic decay of the current in 1D via phase slips is reminiscent of the stochastic decay due to vortex-antivortex recombination in 2D or 3D systems [20], where (however) oscillations are strongly damped by vortex creation [21]. The main difference between the 1D and the higher-dimensional counterparts is that, in the former case, the current dynamics are more robust: at weak interactions, the soliton properties are gradually degraded by the several interactions with the barrier, mainly by sound wave radiation [61]; at strong interactions, we observe the coherent dynamics of all particles. In the outlook, it would be very interesting to investigate how the self-trapping disappears for large but finite interactions, as well as to study the crossover to a quasi-1D geometry to explore the role of radial modes in the decay dynamics.

We thank Maxim Olshanii and Jook Walraven for stimulating discussions. We acknowledge financial support from the ANR project SuperRing (Grant No. ANR-15-CE30-0012). The Laboratoire de Physique des Lasers is a member of DIM SIRTEQ (Science et Ingénierie en Région Île-de-France pour les Technologies Quantiques).

*Corresponding author.

juan.polo@lpmmc.cnrs.fr

- [1] A. Ramanathan, K. C. Wright, S. R. Muniz, M. Zelan, W. T. Hill, C. J. Lobb, K. Helmersen, W. D. Phillips, and G. K. Campbell, *Phys. Rev. Lett.* **106**, 130401 (2011).
- [2] S. Moulder, S. Beattie, R. P. Smith, N. Tammuz, and Z. Hadzibabic, *Phys. Rev. A* **86**, 013629 (2012).
- [3] D. Husmann, S. Uchino, S. Krinner, M. Lebrat, T. Giamarchi, T. Esslinger, and J.-P. Brantut, *Science* **350**, 1498 (2015).
- [4] A. C. Mathey and L. Mathey, *New J. Phys.* **18**, 055016 (2016).
- [5] B. T. Seaman, M. Krämer, D. Z. Anderson, and M. J. Holland, *Phys. Rev. A* **75**, 023615 (2007).
- [6] L. Amico, D. Aghamalyan, F. Aukstol, H. Crepaz, R. Dumke, and L. C. Kwek, *Sci. Rep.* **4**, 4298 (2014).
- [7] L. Amico, G. Birkl, M. Boshier, and L.-C. Kwek, *New J. Phys.* **19**, 020201 (2017).
- [8] G. Gauthier, S. S. Szigeti, M. T. Reeves, M. Baker, T. A. Bell, H. Rubinsztein-Dunlop, M. J. Davis, and T. W. Neely, *arXiv:1903.04086*.
- [9] R. Dumke, Z. Lu, J. Close, N. Robins, A. Weis, M. Mukherjee, G. Birkl, C. Hufnagel, L. Amico, M. G. Boshier, K. Dieckmann, W. Li, and T. C Killian, *J. Opt.* **18**, 093001 (2016).
- [10] K. W. Madison, F. Chevy, V. Bretin, and J. Dalibard, *Phys. Rev. Lett.* **86**, 4443 (2001).
- [11] A. A. Penckwitt, R. J. Ballagh, and C. W. Gardiner, *Phys. Rev. Lett.* **89**, 260402 (2002).
- [12] C. Lobo, A. Sinatra, and Y. Castin, *Phys. Rev. Lett.* **92**, 020403 (2004).
- [13] R. Dubessy, T. Liennard, P. Pedri, and H. Perrin, *Phys. Rev. A* **86**, 011602(R) (2012).
- [14] K. C. Wright, R. B. Blakestad, C. J. Lobb, W. D. Phillips, and G. K. Campbell, *Phys. Rev. A* **88**, 063633 (2013).
- [15] K. C. Wright, R. B. Blakestad, C. J. Lobb, W. D. Phillips, and G. K. Campbell, *Phys. Rev. Lett.* **110**, 025302 (2013).
- [16] S. Eckel, J. G. Lee, F. Jendrzejewski, N. Murray, C. W. Clark, C. J. Lobb, W. D. Phillips, M. Edwards, and G. K. Campbell, *Nature (London)* **506**, 200 (2014).
- [17] A. I. Yakimenko, K. O. Isaeva, S. I. Vilchinskii, and E. A. Ostrovskaya, *Phys. Rev. A* **91**, 023607 (2015).
- [18] A. Muñoz Mateo, A. Gallemí, M. Guilleumas, and R. Mayol, *Phys. Rev. A* **91**, 063625 (2015).
- [19] A. Kumar, S. Eckel, F. Jendrzejewski, and G. K. Campbell, *Phys. Rev. A* **95**, 021602(R) (2017).
- [20] F. Piazza, L. A. Collins, and A. Smerzi, *Phys. Rev. A* **80**, 021601(R) (2009).
- [21] A. C. Mathey, C. W. Clark, and L. Mathey, *Phys. Rev. A* **90**, 023604 (2014).
- [22] M. Kunimi and I. Danshita, *Phys. Rev. A* **95**, 033637 (2017).
- [23] A. Burchianti, F. Scazza, A. Amico, G. Valtolina, J. A. Seman, C. Fort, M. Zaccanti, M. Inguscio, and G. Roati, *Phys. Rev. Lett.* **120**, 025302 (2018).
- [24] K. Khani, E. Neri, L. Galantucci, F. Scazza, A. Burchianti, K. L. Lee, C. F. Barenghi, A. Trombettoni, M. Inguscio, M. Zaccanti, G. Roati, and N. P. Proukakis, *arXiv:1905.08893*.
- [25] I. Danshita and A. Polkovnikov, *Phys. Rev. A* **85**, 023638 (2012).
- [26] C. D'Errico, S. S. Abbate, and G. Modugno, *Phil. Trans. R. Soc. A* **375**, 20160425 (2017).
- [27] L. Tanzi, S. Scaffidi Abbate, F. Cataldini, L. Gori, E. Lucioni, M. Inguscio, G. Modugno, and C. D'Errico, *Sci. Rep.* **6**, 25965 (2016).
- [28] A. Y. Cherny, J.-S. Caux, and J. Brand, *Phys. Rev. A* **80**, 043604 (2009).
- [29] L. D. Carr, C. W. Clark, and W. P. Reinhardt, *Phys. Rev. A* **62**, 063610 (2000).
- [30] M. Cominotti, D. Rossini, M. Rizzi, F. Hekking, and A. Minguzzi, *Phys. Rev. Lett.* **113**, 025301 (2014).
- [31] E. Shamriz and B. A. Malomed, *Phys. Rev. E* **98**, 052203 (2018).
- [32] V. Hakim, *Phys. Rev. E* **55**, 2835 (1997).
- [33] J. A. Freire, D. P. Arovas, and H. Levine, *Phys. Rev. Lett.* **79**, 5054 (1997).
- [34] G. C. Katsimiga, S. I. Mistakidis, G. M. Koutentakis, P. G. Kevrekidis, and P. Schmelcher, *Phys. Rev. A* **98**, 013632 (2018).
- [35] S. Khlebnikov, *Phys. Rev. A* **71**, 013602 (2005).
- [36] J. Polo, V. Ahufinger, F. W. J. Hekking, and A. Minguzzi, *Phys. Rev. Lett.* **121**, 090404 (2018).
- [37] K. V. Kheruntsyan, D. M. Gangardt, P. D. Drummond, and G. V. Shlyapnikov, *Phys. Rev. Lett.* **91**, 040403 (2003).
- [38] A. Kumar, R. Dubessy, T. Badr, C. De Rossi, M. de Goër de Herve, L. Longchambon, and H. Perrin, *Phys. Rev. A* **97**, 043615 (2018).
- [39] A. Smerzi, S. Fantoni, S. Giovanazzi, and S. R. Shenoy, *Phys. Rev. Lett.* **79**, 4950 (1997).
- [40] M. J. Davis, S. A. Morgan, and K. Burnett, *Phys. Rev. Lett.* **87**, 160402 (2001).

- [41] P. B. Blakie, A. S. Bradley, M. J. Davis, R. Ballagh, and C. W. Gardiner, *Adv. Phys.* **57**, 363 (2008).
- [42] N. G. Berloff, M. Brachet, and N. P. Proukakis, *Proc. Natl. Acad. Sci. U.S.A.* **111**, 4675 (2014).
- [43] M. Girardeau, *J. Math. Phys. (N.Y.)* **1**, 516 (1960).
- [44] M. D. Girardeau and E. M. Wright, *Phys. Rev. Lett.* **84**, 5691 (2000).
- [45] V. I. Yukalov and M. D. Girardeau, *Laser Phys. Lett.* **2**, 375 (2005).
- [46] The calculation for $\ell = 2$ yields no qualitative difference in the current dynamics: just a faster decay of the oscillations.
- [47] M. Albiez, R. Gati, J. Fölling, S. Hunsmann, M. Cristiani, and M. K. Oberthaler, *Phys. Rev. Lett.* **95**, 010402 (2005).
- [48] See Supplemental Material at <http://link.aps.org/supplemental/10.1103/PhysRevLett.123.195301> for details, which includes Refs. [49–56].
- [49] M. Brachet, *C.R. Phys.* **13**, 954 (2012).
- [50] C. W. Gardiner, J. R. Anglin, and T. I. A. Fudge, *J. Phys. B* **35**, 1555 (2002).
- [51] C. W. Gardiner and M. J. Davis, *J. Phys. B* **36**, 4731 (2003).
- [52] G. Krstulovic and M. Brachet, *Phys. Rev. E* **83**, 066311 (2011).
- [53] K. Millard, *J. Math. Phys. (N.Y.)* **10**, 7 (1969).
- [54] K. K. Das, M. D. Girardeau, and E. M. Wright, *Phys. Rev. Lett.* **89**, 170404 (2002).
- [55] D. Ananikian and T. Bergeman, *Phys. Rev. A* **73**, 013604 (2006).
- [56] V. O. Nesterenko, A. N. Novikov, and E. Suraud, *Laser Phys.* **24**, 125501 (2014).
- [57] B. M. Caradoc-Davies, R. J. Ballagh, and K. Burnett, *Phys. Rev. Lett.* **83**, 895 (1999).
- [58] For the sake of clarity, we plot only the density deviations with respect to the time-averaged value.
- [59] We fit all the datasets with the same model: $J(t) = Ae^{-\Gamma_A t} + B \cos[\omega t + \phi]e^{-\Gamma_B t}$ allows us to capture both a simple exponential decay and damped oscillations. This model also works remarkably well in the intermediate regime where the two effects are simultaneously present.
- [60] T. Karpiuk, P. Deuar, P. Bienias, E. Witkowska, K. Pawłowski, M. Gajda, K. Rzążewski, and M. Brewczyk, *Phys. Rev. Lett.* **109**, 205302 (2012).
- [61] N. Bilas and N. Pavloff, *Phys. Rev. A* **72**, 033618 (2005).
- [62] O. V. Astafiev, L. B. Ioffe, S. Kafanov, Y. A. Pashkin, K. Y. Arutyunov, D. Shahar, O. Cohen, and J. S. Tsai, *Nature (London)* **484**, 355 (2012).
- [63] J. E. Mooij and Y. V. Nazarov, *Nat. Phys.* **2**, 169 (2006).
- [64] L. Corman, L. Chomaz, T. Bienaimé, R. Desbuquois, C. Weitenberg, S. Nascimbène, J. Dalibard, and J. Beugnon, *Phys. Rev. Lett.* **113**, 135302 (2014).
- [65] S. Eckel, F. Jendrzejewski, A. Kumar, C. J. Lobb, and G. K. Campbell, *Phys. Rev. X* **4**, 031052 (2014).
- [66] G. E. Marti, R. Olf, and D. M. Stamper-Kurn, *Phys. Rev. A* **91**, 013602 (2015).
- [67] A. Kumar, N. Anderson, W. D. Phillips, S. Eckel, G. K. Campbell, and S. Stringari, *New J. Phys.* **18**, 025001 (2016).